International Journal of
Environmental Research and Public Health

MDPI

Article

Factors Influencing O_3 Concentration in Traffic and Urban Environments: A Case Study of Guangzhou City

Tao Liu [1,2,†], Jia Sun [3,†], Baihua Liu [1,2], Miao Li [1,*], Yingbin Deng [2,3,*], Wenlong Jing [2,3] and Ji Yang [2,3]

1 College of Geographical Science, Harbin Normal University, Harbin 150025, China
2 Guangdong Open Laboratory of Geospatial Information Technology and Application, Lab of Guangdong for Utilization of Remote Sensing and Geographical Information System, Guangzhou Institute of Geography, Guangdong Academy of Sciences, Guangzhou 510070, China
3 Southern Marine Science and Engineering Guangdong Laboratory (Guangzhou), Guangzhou 511485, China
* Correspondence: mli@hrbnu.edu.cn (M.L.); yingbin@gdas.ac.cn (Y.D.)
† These authors contributed equally to this work.

Abstract: Ozone (O_3) pollution is a serious issue in China, posing a significant threat to people's health. Traffic emissions are the main pollutant source in urban areas. NO_X and volatile organic compounds (VOCs) from traffic emissions are the main precursors of O_3. Thus, it is crucial to investigate the relationship between traffic conditions and O_3 pollution. This study focused on the potential relationship between O_3 concentration and traffic conditions at a roadside and urban background in Guangzhou, one of the largest cities in China. The results demonstrated that no significant difference in the O_3 concentration was observed between roadside and urban background environments. However, the O_3 concentration was 2 to 3 times higher on sunny days (above 90 $\mu g/m^3$) than on cloudy days due to meteorological conditions. The results confirmed that limiting traffic emissions may increase O_3 concentrations in Guangzhou. Therefore, the focus should be on industrial, energy, and transportation emission mitigation and the influence of meteorological conditions to minimize O_3 pollution. The results in this study provide some theoretical basis for mitigation emission policies in China.

Keywords: ozone; nitrogen dioxide; traffic condition; impact factors

check for updates

Citation: Liu, T.; Sun, J.; Liu, B.; Li, M.; Deng, Y.; Jing, W.; Yang, J. Factors Influencing O_3 Concentration in Traffic and Urban Environments: A Case Study of Guangzhou City. *Int. J. Environ. Res. Public Health* **2022**, *19*, 12961. https://doi.org/10.3390/ijerph191912961

Academic Editor: Paul B. Tchounwou

Received: 26 August 2022
Accepted: 6 October 2022
Published: 10 October 2022

1. Introduction

Air pollution has become a crucial issue in China due to rapid economic development [1]. The Chinese government has exerted a significant effort to reduce air pollution in recent years. As a result, fine particulate matter ($PM_{2.5}$) has significantly decreased due to strict emission mitigation policies [2]. Ozone (O_3) has become the most prevalent pollutant in China. The O_3 concentration has increased by 10.6% from 2015 to 2021 in 339 [3,4]. Excessive exposure to O_3 can be extremely harmful to human health, causing substantial damage and irritation to the eyes, respiratory tract, and lungs [5–7].

Many studies have focused on O_3 pollution in China, investigating the spatiotemporal variations [8–12], secondary formation mechanism [13–15], emission sources [16–19], and other factors. The Pearl River Delta (PRD) is one of the most developed regions in China and has experienced significant O_3 pollution. The O_3 concentration has increased in the PRD since 2015 [20]. The O_3 pollution is the highest in autumn in the PRD due to high temperatures, strong solar radiation, and low relative humidity (RH) [21–25]. In addition, several studies confirmed the "weekend effect" [26,27] in China, i.e., the O_3 concentration is higher on weekends than during working days in Beijing [28], Shanghai [29,30], and Guangzhou [31]. There are two reasons. First, the nitric oxide (NO) concentration is lower during the weekend due to fewer traffic emissions. Therefore, the inhibitory effect of NO on O_3 is weaker, and more O_3 is generated. Second, fewer aerosol particles are emitted during the weekend, resulting in less scattering and absorption of solar radiation. As a result, more O_3 is formed due to the stronger solar radiation during weekends [32].

There are three major sources of near-ground O_3 precursors: traffic emissions [33], industry emissions, and emissions by power plants [34]. Mitigating O_3 pollution has become a crucial issue in the PRD region in recent years [35]. However, it is challenging to control O_3 pollution due to the complex O_3 generation mechanism [36]. After absorbing ultraviolet light, tropospheric O_2 decomposes into two O atoms. The O atoms are combined with O_2 to form O_3 (Equations (1) and (2)). In urban areas, NO_2 in traffic emissions is the main precursor of O_3 (Equation (3)). O_3 rapidly oxidize NO to form NO_2, known as the titration effect (Equation (4)).

$$O_2 + UV \rightarrow O + O \tag{1}$$

$$O + O_2 + M \rightarrow O_3 + M \tag{2}$$

$$NO_2 + hv \rightarrow NO + O \tag{3}$$

$$O_3 + NO \rightarrow NO_2 + O_2 \tag{4}$$

In these processes, a dynamic equilibrium exists during the formation and consumption of O_3 by NO_X. However, alkoxy radicals (RO) and hydroperoxyl radicals (HO_2) generated by the reaction of volatile organic compounds (VOCs) and hydroxyl (OH) radicals in the atmosphere also react with NO (Equations (5)–(8)), destroying the dynamic balance between NO_X and O_3 and increasing the O_3 concentration.

$$HO_2 + NO \rightarrow HO + NO_2 \tag{5}$$

$$RO_2 + NO \rightarrow RO + NO_2 \tag{6}$$

$$HO + RH + O_2 \rightarrow RO_2 + H_2O \tag{7}$$

$$RO + O_2 + hv \rightarrow HO_2 + RCHO \tag{8}$$

If large amounts of NO_X are emitted, HO and RO_2 react predominantly with NO_2 (Equations (9) and (10)); if small amounts of NO_X are emitted, the free radical reaction dominates (Equations (11) and (12)). According to the formation mechanism of O_3, the O_3 concentration is closely related to the NO_X and VOCs concentrations because of the highly nonlinear relationship between O_3 and its precursors. Therefore, it is more difficult to mitigate O_3 than other pollutants.

$$RO_2 + NO_2 \rightarrow RO_2NO_2 \tag{9}$$

$$HO + NO_2 \rightarrow HNO_3 \tag{10}$$

$$HO_2 + HO_2 \rightarrow H_2O_2 + O_2 \tag{11}$$

$$HO_2 + RO_2 \rightarrow RO_2H + O_2 \tag{12}$$

The O_3 concentration depends on the O_3 formation process and diffusion [37–39]. Accordingly, the photochemical reaction rate [40], human activities, and meteorological conditions are the three dominant factors affecting the local O_3 concentration [41,42]. Many studies have demonstrated that low cloudiness [43,44], intense solar radiation [45], high temperature [46,47], and low RH [48] can accelerate the O_3 production rate [49,50]. High road network density [51], frequent motor vehicle braking, rapid acceleration, and high traffic flow [52] lead to high NO_X emissions [53]. Wind speed and direction can affect the horizontal distribution of O_3 in local areas, and a low wind speed facilitates O_3 accumulation [54,55].

Traffic emissions are the main pollutant source in urban areas. NO_X and VOC from traffic emissions are the main precursors of O_3. Therefore, it is necessary to investigate the relationship between traffic conditions and O_3 pollution. However, there are very few studies focusing on the influence of traffic situations on O_3. We investigate the potential relationship between the O_3 concentration and traffic conditions at roadside and urban background stations in Guangzhou, one of the largest cities in the PRD and China. The results provide a scientific reference for policymakers to establish emission mitigation policies.

2. Materials and Methods

2.1. Study Area and Measurement Data

Guangzhou is one of the largest cities in China, with a developed economy, dense population, and advanced manufacturing industries. The atmospheric pollutant concentrations were obtained from three national monitoring stations: two roadside stations (Yangji station (YJ station) and Huangsha station (HS station)) and one urban background station (Luhu station (LH station)) (Figure 1). The YJ station is located at an intersection of the main road (Zhongshan road) in the city center, about 5 m higher above ground. The HS station is located on a three-layer viaduct. The measurement instruments were installed between the second and third layers, about 20 m above the ground. The LH station is situated in Luhu Park, allowing us to compare air pollution in traffic and an urban park. The national measurement data were obtained from Guangzhou Ecological Environment Bureau (http://sthjj.gz.gov.cn/, accessed on 1 July 2021). The temporal resolution of the measurement data is one hour.

Meteorological data were obtained from Guangzhou Weather website (http://www.tqyb.com.cn/gz/weatherLive/autoStation/, accessed on 1 July 2021), including ambient temperature, wind speed, wind direction, solar radiation, and RH. The dynamic traffic data were obtained from the Guangzhou Municipal Bureau of Transportation (http://jtj.gz.gov.cn/jtcx/lkcx/, accessed on 1 July 2021). All the data were quality-controlled and covered the period from January to June 2021.

2.2. Analysis Approaches

A stepwise regression model was used to investigate the relationship between the potential impact factors and O_3 concentration. Stepwise regression analysis automatically selects the most important variables to establish a predictive or explanatory model. The influencing factor are incorporated into the model one by one, and the statistical significance was evaluated. The insignificant factors were removed from the model.

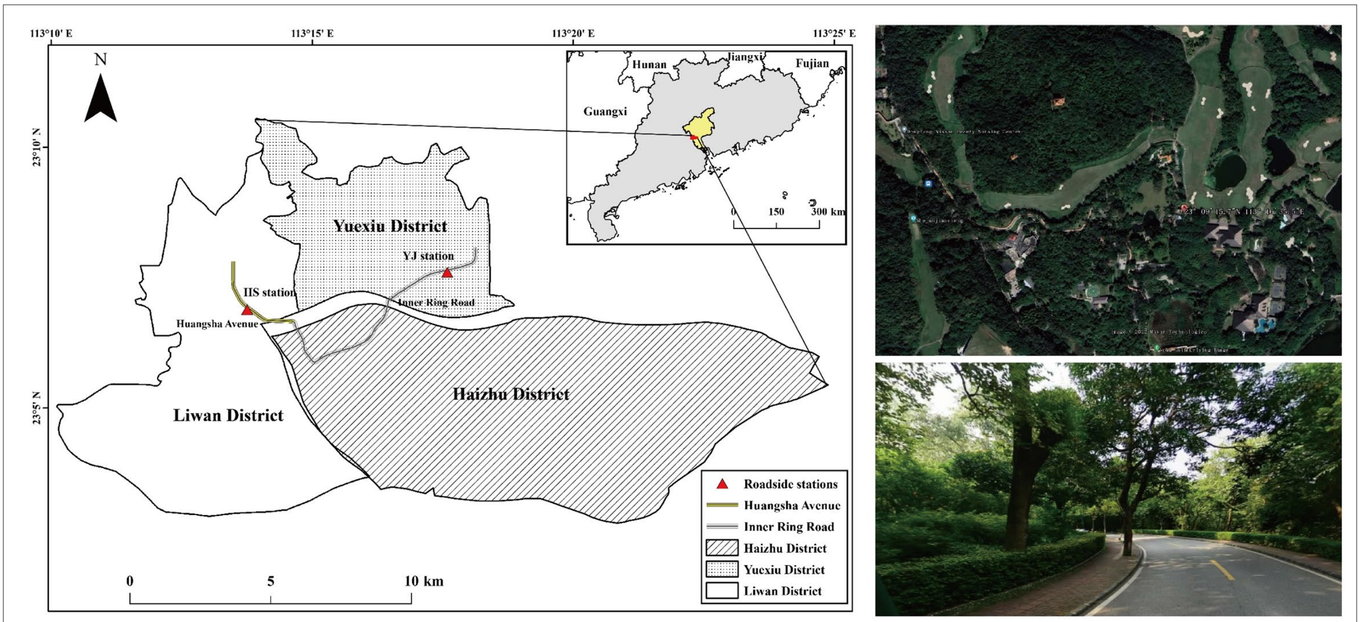

(a) (b)

Figure 1. *Cont.*

Figure 1. Overview of the study area and atmospheric monitoring stations. (**a**) Location of three stations; (**b**) Luhu station (LH); (**c**) Huangsha station (HS); (**d**) Yangji station (YJ).

3. Results and Discussion

3.1. Temporal Variations of NO_2 and O_3

3.1.1. Daily Variations

Generally, pollutant concentrations are affected by several factors, such as emission sources, meteorological conditions, and pollutant formation mechanisms. The median diurnal variation of O_3 and NO_2 during the cold (from January to March) and warm (from April to June) seasons is shown in Figure 2. Similar diurnal patterns of O_3 are observed at the three stations. The O_3 concentration is low from 22:00 to the early morning on the following day. Then, it rapidly increases from around 8:00 in the morning and reaches the maximum around 14:00–16:00. As the solar radiation increases during the daytime, the O_3 concentration increases [56,57] (Equations (1) and (2)). However, the O_3 concentration remains low during the night. There are two reasons. First, less O_3 is generated in the absence of sunlight. Second, NO can react with O_3 to form NO_2 and O_2 during the night (Equation (4)), which is referred to as the titration effect of NO.

The diurnal variation of NO_2 differs from that of O_3. As shown in Figure 2d–f, the NO_2 concentration is lower at 3:00–4:00 and 12:00–16:00 and higher at 6:00–8:00 and 20:00–22:00. The highest NO_2 concentration occurs at 20:00–22:00. The NO_2 concentration shows an increasing trend from 04:00–8:00 at the two roadside stations (HS and JY) because of traffic emissions. This increasing trend is not observed at the urban background station (LH). The solar radiation increases after 08:00. NO_2 reacts with VOCs to produce O_3, resulting in a decreasing trend at all three stations. The NO_2 concentration increases after 16:00 due to lower solar radiation and a decrease in the photochemical reaction [58–60]. During the night, the NO_2 concentration increases again due to the titration effect [61].

The seasonal difference in the pollutant concentration is larger for NO_2 than for O_3, as shown in Figure 2d–f. The NO_2 concentration is higher in the cold season (from January to March) than in the warm season (from April to June). The decisive factor influencing the seasonal variation of the NO_2 concentration is solar radiation. The average solar radiance in Guangzhou is 1352 kJ/ m^2 in the cold season and 1806 kJ/ m^2 in the warm season. Lower solar radiation leads to less O_3 generation and less NO_2 consumption. Another possible factor may be the lower RH in winter. In Guangzhou, the average RH is 59.04% and 86.2% in the cold and warm seasons, respectively [62,63]. A higher RH results in a stronger photochemical reaction and a lower NO_2 concentration in the warm season. Another possible explanation is the seasonal change in the planetary boundary layer height. It is 717 m in winter and 1239 m in summer in Guangzhou [64,65]. A lower planetary boundary layer accumulates NO_2, resulting in a higher NO_2 concentration [66]. However, the seasonal difference in the O_3 concentration is smaller than that of the NO_2 concentration. The reason is that O_3 is a secondary pollutant whose concentration is controlled by highly complex and nonlinear secondary formation mechanisms.

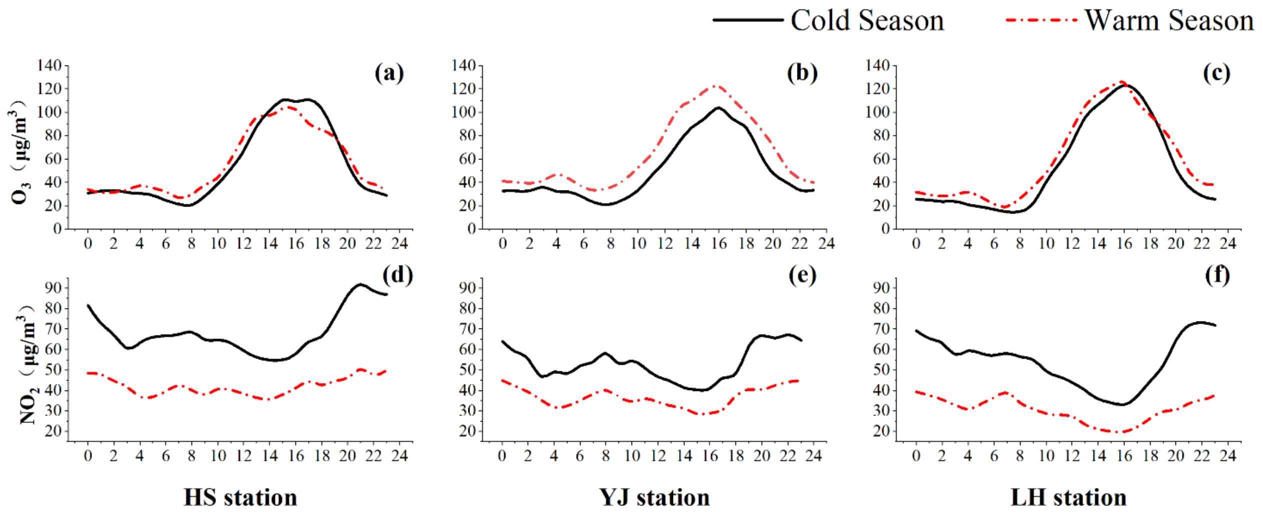

Figure 2. Diurnal variation of typical pollutants in cold and warm seasons: O_3 concentrations at (**a**) HS station, (**b**) YJ station, and (**c**) LH station; NO_2 concentrations at (**d**) HS station, (**e**) YJ station, and (**f**) LH station.

3.1.2. Weekly Variations

The weekly variations in the O_3 and NO_2 concentrations at the three stations are illustrated in Figure 3. In general, the weekly trends of the O_3 and NO_2 concentrations are similar at three stations, but the average concentrations are different. As shown in Figure 3a, the O_3 concentration is significantly higher on weekends (Saturday and Sunday) than on weekdays (from Monday to Friday), indicating the weekend effect of O_3. It is believed to be related to a change in the proportion of O_3 precursor emissions and other pollutant emissions from human activities [67]. Fewer human activities on weekends lead to lower $PM_{2.5}$ and a lower aerosol optical thickness and radiation extinction. Therefore, the O_3 concentrations are higher on the weekend than on weekdays due to stronger photochemical reactions [68,69]. Moreover, high traffic flow during the morning rush hour results in a rapid increase in the NO concentration, inhibiting O_3 formation on weekdays [70,71].

Differences in the O_3 concentration are observed at the three stations. The highest O_3 concentration was measured at the LH station, followed by the two roadside stations YJ and HS. The reason is the surrounding environment. The LH station is located in Luhu Park. VOCs generated by biological sources compete with NO, reducing the inhibition of NO on O_3 and leading to a higher O_3 concentration [72,73]. The YJ station is surrounded mostly by business and entertainment areas with frequent human activities. Large amounts of NO_X are emitted from traffic inhibited O_3 formation. In addition, the titration effect of NO is stronger at the YJ station, leading to a slightly lower O_3 concentration at the YJ station than at the LH station. The HS station is a roadside station located near a park. It has higher vegetation cover than the YJ station.

The weekly variation in the NO_2 concentration shows a significantly different pattern than that of the O_3 concentration. The NO_2 concentration is slightly higher on weekdays than on the weekend due to higher anthropogenic emissions, especially traffic emissions in urban areas [74–77]. The NO_2 concentration is the highest at the HS station, followed by the

YJ and LH stations, which is consistent with the traffic emissions and the local environment of the three stations.

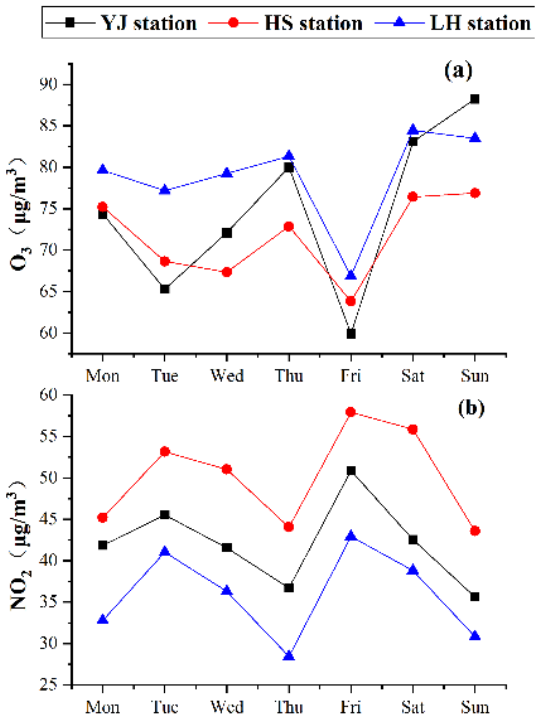

Figure 3. Weekly variation in O_3 (**a**) and NO_2 (**b**) concentrations at the three stations.

3.2. Influencing Factors

3.2.1. Synergistic Variation of O_3 and NO_2

Figure 4 shows the scatterplots of the O_3 and NO_2 concentrations during the daytime (07:00–19:00) and nighttime (20:00–06:00) at the three stations. The linear regression model has a negative slope for all three stations during the daytime and nighttime, indicating that the NO_2 concentration decreases as the O_3 concentration increases. However, differences are observed between daytime and nighttime. In the daytime, NO_2 is consumed, and O_3 is produced (Equations (2) and (3)). However, without a photochemical reaction during nighttime, O_3 is converted to NO_2 due to the titration effect (Equation (4)), leading to a lower O_3 concentration. Due to the highly nonlinear and complex O_3 formation mechanism, the R^2 value is low for all fitting results. The R^2 value is larger during nighttime at all three stations due to the absence of the photochemical reaction, the titration effect of NO, and weaker vertical diffusion [78,79]. The nighttime fitting degree is better at the LH station than at the roadside stations. The reason might be the surrounding environment of the LH station. The vegetation cover is higher; thus, vegetation respiration is stronger at night. Consequently, the NO_2 and O_3 concentrations are relatively stable, leading to a better fitting degree.

The fitted results of the three stations are similar. However, the dominant emission sources differ at the three stations. This result indicates no significant effect of traffic emissions on the O_3 concentration at the roadside stations. Due to the absence of VOCs, a dynamic equilibrium exists between O_3 and NO_X in the atmosphere. Thus, O_3 is not accumulated and does not exceed the air pollution standard [80,81]. However, the reaction between VOCs and NO weakens the inhibitory effect of NO on O_3, resulting in high O_3 pollution [82]. Controlling NO_X emissions does not mitigate O_3 pollution. Moreover, Guangzhou is in the VOC-limitation area [83,84]. Limiting vehicle emissions to reduce the NO_X concentration may even increase the O_3 concentration. Therefore, the focus should be on industrial, energy, and transportation emission mitigation and the influence of meteorological conditions to minimize O_3 pollution.

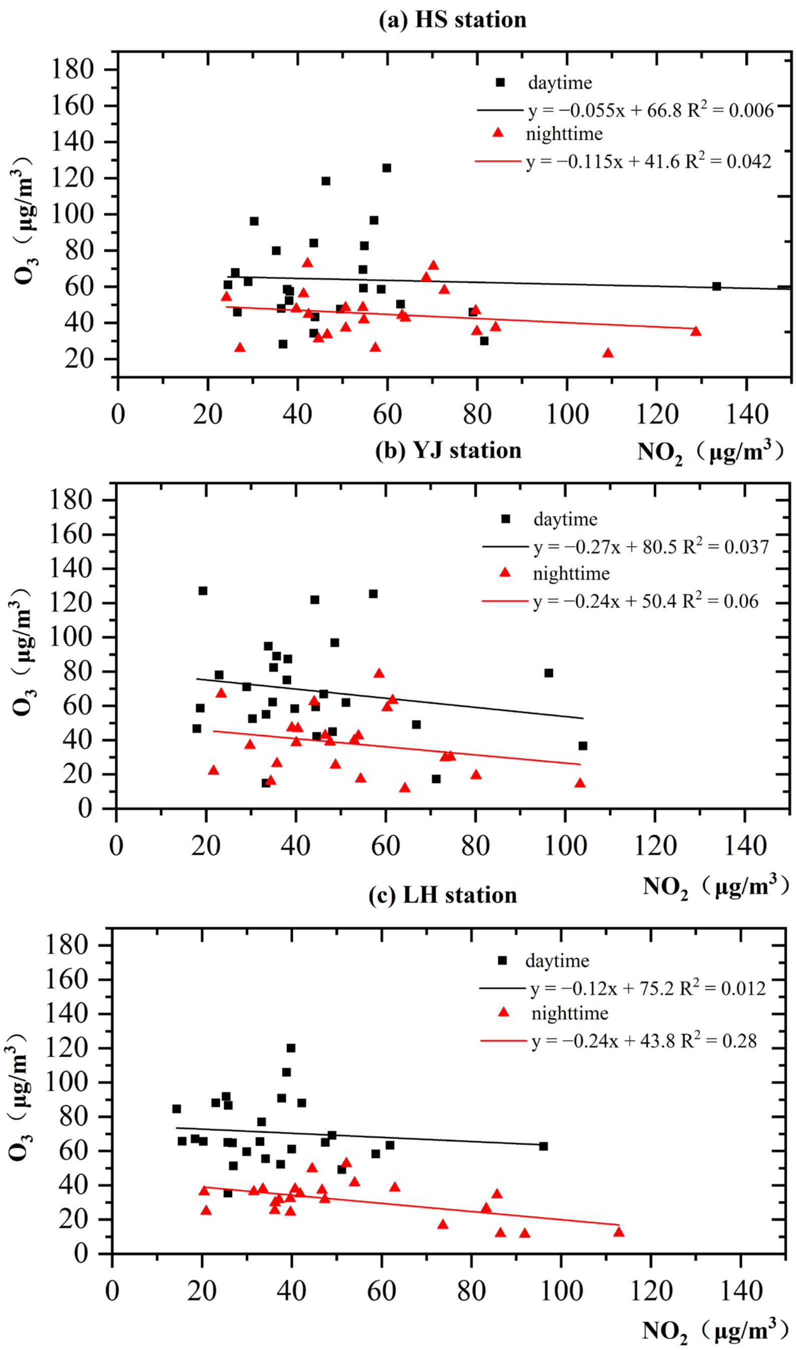

Figure 4. Scatterplot of O_3 and NO_2 concentrations at HS (**a**), YJ (**b**), and LH (**c**).

3.2.2. Pearson Correlation and Stepwise Regression Analyses

Pearson correlation analysis and stepwise regression analysis were conducted to describe the relationship between the pollutant concentration and other factors, such as meteorological parameters and dynamic traffic parameters. Tables 1 and 2 show the results of Pearson's correlation analysis and stepwise regression analysis, respectively. Pearson's correlation shows the correlation between the O_3 concentration and potential factors, and the stepwise regression model determines the significant impact factors. The beta values are used to quantify the contribution of the variables. Briefly, the O_3 concentration is positively correlated with solar radiation, temperature, and travel-time ratio and negatively correlated with the NO_2 concentration, wind speed, and vehicle speed (Table 1). The stepwise regression model shows that the significant factors affecting O_3 concentration are temperature, NO_2 concentration, and RH. As shown in Table 1, the O_3 concentration positively correlates with the travel-time ratio. The travel time ratio is the ratio of the actual travel time to the ideal travel time in smooth traffic flow. The larger the ratio, the higher the degree of traffic congestion. The NO_X and VOC emissions are higher during frequent vehicle braking than during uniform driving. Thus, more O_3 precursors are emitted, leading to a significant positive correlation between O_3 concentration and travel-time ratio. The temperature is positively correlated with O_3 concentration as a result of O_3 formation. The negative correlation between the NO_2 and O_3 concentrations has already been discussed in Section 3.2.1. Moreover, a negative correlation is observed between vehicle speed and O_3 concentration. The fuel consumption is higher at higher speeds than at lower speeds, resulting in more precursor emissions and a higher O_3 concentration. Wind speed and O_3 concentration are negatively correlated because of the dilution effect. The O_3 concentration is lower at higher RH due to wet deposition. Moreover, an increase in RH significantly reduces the number of oxygen atoms, reducing the amount of O_3 generation.

Table 1. Pearson's correlation coefficients between O_3 concentration and various factors.

Impact Factors	Daytime	Nighttime
Temperature (°C)	0.047 **	0.057 **
Wind speed (m/s)	−0.082 **	−0.057 **
Daily precipitation (mm)	**−0.101** **	−0.006
Vehicle speed (m/s)	**−0.111** **	**−0.111** **
Travel-time ratio	**0.150** **	**0.129** **
NO_2 (μg/m^3)	−0.220 *	−0.153 **
RH (%)	**−0.495** **	**−0.226** **
Solar radiation (J/m^2)	**0.448** **	**0.279** **

** Significant at the 0.01 level. * Significant at the 0.05 level.

Table 2. Results of stepwise regression model between O_3 concentration and various factors.

Model	Daytime	p	Nighttime	p
	Beta Value		Beta Value	
Temperature (°C)	0.386	0.000	0.207	0.000
Wind speed (m/s)	−0.076	0.000	−0.124	0.000
Daily precipitation (mm)	0.092	0.000	0.036	0.037
Vehicle speed (m/s)	−0.077	0.000	−0.063	0.000
NO_2 (μg/m^3)	−0.407	0.000	−0.611	0.000
RH (%)	−0.578	0.000	−0.389	0.000
Solar radiation (J/m^2)	-	-	0.182	0.000

The dependent variable: O_3 (μg/m^3).

The secondary pollutant O_3 is correlated with several factors. The vehicle speed and travel-time ratio are significantly correlated with the O_3 concentration, indicating the importance of traffic emissions on O_3 pollution in urban areas.

3.2.3. Case Study

As discussed in the previous section, traffic emissions affect the O_3 concentration but are not the dominant factor. Many studies demonstrated that solar radiation was a significant factor influencing O_3 formation. A case study was conducted to quantify the influence of solar radiation on O_3 concentration in Guangzhou. Two weeks were selected: 1 February to 7 February 2021, with sunny weather, and 24 February to 2 March 2021, with cloudy weather.

The pollutant concentrations and related parameters are listed in Table 3. The O_3 concentration is substantially different on sunny and cloudy days at all three stations, indicating the predominant influence of solar radiation. The O_3 concentration is 2–3 times higher on sunny days than on cloudy days in the daytime and nighttime. However, there are no large differences in the NO_2 concentration. In the daytime, there are no differences in the NO_2 concentration between sunny and cloudy days. However, the nighttime NO_2

concentration is 1.5 to 2 times higher on sunny days than on cloudy days. More O_3 is formed during sunny days, leading to a stronger titration effect and a higher NO_2 concentration during the nighttime on sunny days. It should be noted that the NO_2 concentration is lower at the LH station than at the two roadside stations during the daytime. However, the O_3 concentration is similar at all three stations due to the lower inhibitory effect of NO, as discussed in Section 3.1.2. This finding confirms our results, i.e., traffic emissions contribute significantly to O_3 generation, but the contribution is not higher at roadside stations than at the urban background station.

Table 3. The pollutant concentrations and related parameters in the two periods.

Period	Station	O_3 (μg/m^3)		NO_2 (μg/m^3)		Travel-Time Ratio		Solar Radiation (KJ/m^2)	RH (%)
		Day Time	Night Time	Day Time	Night Time	Day Time	Night Time		
Sunny days	HS	97.43	52.95	54.28	79.05	1.14	1.03	17,627.04	64.71%
	JY	94.70	63.45	48.80	63.66	1.25	1.06		
	LH	102.31	45.88	38.87	79.34	-	-		
Cloudy days	HS	37.30	21.15	52.34	53.10	1.21	1.05	10,300.89	75.08%
	JY	42.90	27.86	46.16	48.26	1.29	1.08		
	LH	41.70	25.75	36.99	41.59	-	-		

The scatterplots of the NO_2 and O_3 concentrations in the two periods at YJ and HS are shown in Figure 5. The colored dots indicate the dynamic traffic conditions. The linear regression results demonstrate that the negative correlation between the NO_2 and O_3 concentrations is stronger during the daytime than during the nighttime at both stations due to the stronger photochemical reaction strength. Furthermore, no significant relationship is observed between the O_3 concentration and dynamic traffic conditions.

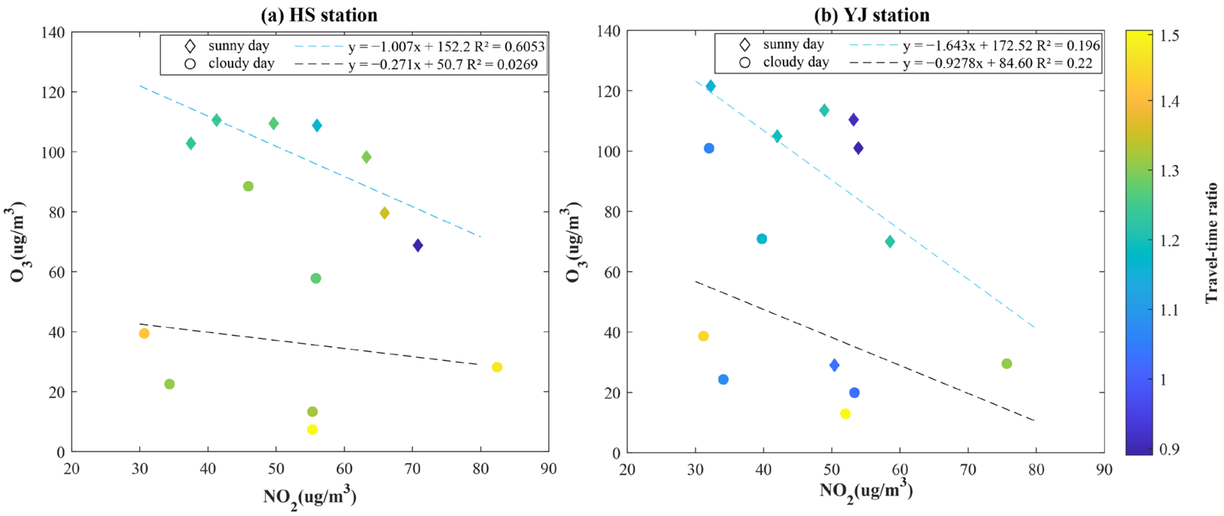

Figure 5. Scatterplot of daily O_3 and NO_2 concentrations in the two periods at the HS (**a**) and YJ (**b**) stations. The colored dots denote the travel-time ratio.

4. Conclusions

This study evaluated the factors influencing the O_3 concentration in traffic and urban background environments. The diurnal and weekly variation of the O_3 and NO_2 concentrations demonstrated a similar pattern at the three stations. These results were attributed to differences in the O_3 generation mechanism, meteorological conditions, and emission sources. However, no significant differences in the O_3 variation were observed between the three stations, implying that the O_3 concentration was not significantly higher in the traffic environment than in the urban background environment. Since Guangzhou is located in a

VOC-limited area, the lower O_3 concentration in the urban background area is due to the lower inhibition of NO on O_3.

Pearson correlation analysis and stepwise regression analysis were used to describe the relationship between the pollutant concentration and the influencing factors, such as meteorological and dynamic traffic parameters. Traffic and meteorological parameters (temperature, solar radiation, RH, and precipitation) were significantly correlated with the O_3 concentration at the two roadside stations. It was concluded that traffic emissions contributed to O_3 pollution in the urban area but were not the decisive factor, while the meteorological factors also influenced the O_3 concentration.

A case study was conducted for two weeks to quantify the influence of solar radiation on O_3 concentration in Guangzhou. On sunny days, the O_3 concentration exceeded 90 $\mu g/m^3$ at the three sites. It was 2 to 3 times higher than during cloudy days due to meteorological conditions. The dynamic traffic condition (travel-time ratio) had no significant relationship with the O_3 and NO_2 concentrations at the two roadside stations.

This study analyzed the temporal variation of O_3 and its precursor NO_2 at roadside and urban background environments in Guangzhou and its influencing factors. The results confirmed that limiting traffic emissions might increase O_3 concentrations in Guangzhou. Therefore, emission mitigation should be performed, i.e., industrial, energy, and transportation emission mitigation, and the influence of meteorological conditions should be considered to minimize O_3 pollution. However, some limitations exist in this study. Due to a lack of NO and VOCs data, the relationship between O_3 concentration and NO and VOCs was not analyzed. In future, a mobile measurement focusing on O_3 will be carried out in Guangzhou, and a more detailed analysis will be performed.

Author Contributions: Data analysis and writing of the original draft: T.L., J.S.; Concept construction and supervision: M.L., Y.D.; Data analysis, review, and editing, B.L., W.J. and J.Y. All authors have read and agreed to the published version of the manuscript.

Funding: This research was fund by the Key Special Project for Introduced Talents Team of Southern Marine Science and Engineering Guangdong Laboratory (Guangzhou), grant number GML2019ZD0301; National Natural Science Foundation of China, grant number 41901372 and 41976189; Science and Technology Program of Guangzhou, grant number 202002030247; the GDAS' Project of Science and Technology Development, grant number 2022GDASZH-2022010202 and the Science and Technology Program of Guangdong, grant number 2021B1212100006.

Institutional Review Board Statement: Not applicable.

Informed Consent Statement: Not applicable.

Data Availability Statement: The data presented in this study are available on request from the corresponding website.

Acknowledgments: We would like to thank the anonymous reviewers for their constructive comments. We also thank the Geographical Science Data Center of The Greater Bay Area for providing the relevant data for this study.

Conflicts of Interest: The authors declare no conflict of interest.

References

1. Zheng, Y.; Peng, J.; Xiao, J.; Su, P.; Li, S. Industrial structure transformation and provincial heterogeneity characteristics evolution of air pollution: Evidence of a threshold effect from China. *Atmos. Pollut. Res.* **2020**, *11*, 598–609. [CrossRef]
2. He, Q.; Zhang, M.; Song, Y.; Huang, B. Spatiotemporal assessment of $PM_{2.5}$ concentrations and exposure in China from 2013 to 2017 using satellite-derived data. *J. Clean. Prod.* **2021**, *286*, 124965. [CrossRef]
3. Liu, D.; Li, J.; Su, X.; Zuo, R. Analysis of ozone sources in Xining based on CAMx-OSAT method. *J. Environ. Sci.* **2021**, *41*, 386–394.
4. Alfoldy, B.; Kotb, M.; Yigiterhan, O.; Safi, M.A.; Giamberini, S. BTEX, nitrogen oxides, ammonia and ozone concentrations at traffic influenced and background urban sites in an arid environment. *Atmos. Pollut. Res.* **2018**, *10*, 445–454. [CrossRef]
5. Wang, X.; Zhao, W.; Li, L.; Yang, X.; Jiang, J.; Sun, S. Spatial and temporal distribution characteristics of ozone in China and its influence on socio-economic factors. *Earth Environ.* **2020**, *48*, 66–75.
6. Lin, H.; An, Q.; Chao, L.; Pun, V.C.; Chi, S.C.; Tian, L. Gaseous air pollution and acute myocardial infarction mortality in Hong Kong: A time-stratified case-crossover study. *Atmos. Environ.* **2013**, *76*, 68–73. [CrossRef]

7. Cacciottolo, M.; Wang, X.; Driscoll, I.; Woodward, N.; Saffari, A.; Reyes, J.; Serre, M.L.; Vizuete, W.; Sioutas, C.; Morgan, T.E. Particulate air pollutants, APOE alleles and their contributions to cognitive impairment in older women and to amyloidogenesis in experimental models. *Transl. Psychiatry* **2017**, *7*, e1022. [CrossRef]
8. Parrish, D.D.; Petropavlovskikh, I.; Oltmans, S.J. Reversal of Long-Term Trend in Baseline Ozone Concentrations at the North American West Coast. *Geophys. Res. Lett.* **2017**, *44*, 10,675–10,681. [CrossRef]
9. Young, P.J.; Naik, V.; Fiore, A.M.; Gaudel, A.; Lewis, A. Tropospheric ozone assessment report: Assessment of global-scale model performance for global and regional ozone distributions, variability, and trends. *Elem. Sci. Anthr.* **2018**, *6*, 10.
10. Tarasick, D.; Galbally, I.E.; Cooper, O.R.; Schultz, M.G.; Neu, J.L. Tropospheric ozone assessment report: Tropospheric ozone from 1877 to 2016, observed levels, trends and uncertainties. *Elem. Sci. Anthr.* **2019**, *7*, 39.
11. Zhang, R.; Lei, W.; Tie, X.; Hess, P. Industrial emissions cause extreme urban ozone diurnal variability. *Proc. Natl. Acad. Sci. USA* **2004**, *101*, 6346–6350. [CrossRef] [PubMed]
12. Zhang, Y.; Shao, K.; Tang, X.; Li, J. Studies on photochemical smog pollution in Chinese cities. *J. Peking Univ. (Nat. Sci. Ed.)* **1998**, *Z1*, 260–268.
13. Ma, W.; Feng, Z.; Zhan, J.; Liu, Y.; Liu, P.; Liu, C.; Ma, Q.; Yang, K.; Wang, Y.; He, H. Influence of photochemical loss of volatile organic compounds on understanding ozone formation mechanism. *Atmos. Chem. Phys.* **2022**, *22*, 4841–4851. [CrossRef]
14. Liu, J.; Li, X.; Tan, Z.; Wang, W.; Zhang, Y. Assessing the Ratios of Formaldehyde and Glyoxal to NO_2 as Indicators of O_3–NO_X –VOC sensitivity. *Environ. Sci. Technol.* **2021**, *55*, 10935–10945. [CrossRef] [PubMed]
15. Zhang, K.; Huang, L.; Li, Q.; Huo, J.; Duan, Y.; Wang, Y.; Yaluk, E.; Wang, Y.; Fu, Q.; Li, L. Explicit modeling of isoprene chemical processing in polluted air masses in suburban areas of the Yangtze River Delta region: Radical cycling and formation of ozone and formaldehyde. *Atmos. Chem. Phys.* **2021**, *21*, 5905–5917. [CrossRef]
16. Ge, S.; Wang, S.; Xu, Q.; Ho, T. Characterization and sensitivity analysis on ozone pollution over the Beaumont-Port Arthur Area in Texas of USA through source apportionment technologies. *Atmos. Res.* **2020**, *247*, 105249. [CrossRef]
17. Liu, Y.; Song, M.; Liu, X.; Zhang, Y.; Hui, L.; Kong, L.; Zhang, Y.; Zhang, C.; Qu, Y.; An, J.; et al. Characterization and sources of volatile organic compounds (VOCs) and their related changes during ozone pollution days in 2016 in Beijing, China. *Environ. Pollut.* **2020**, *257*, 113599. [CrossRef]
18. Wang, H.; An, J.; Shen, L.; Zhu, B.; Pan, C.; Liu, Z.; Liu, X.; Duan, Q.; Liu, X.; Wang, Y. Mechanism for the formation and microphysical characteristics of submicron aerosol during heavy haze pollution episode in the Yangtze River Delta, China. *Sci. Total Environ.* **2014**, *490*, 501–508. [CrossRef]
19. Shen, L.; Wang, H.; Zhu, B.; Zhao, T.; Wang, Y. Impact of urbanization on air quality in the Yangtze River Delta during the COVID-19 lockdown in China. *J. Clean. Prod.* **2021**, *296*, 126561. [CrossRef]
20. Xiao, L.; Hong, J.; Lin, Z.; Cooper, O.R.; Schultz, M.G.; Xu, X.; Tao, W.; Gao, M.; Zhao, Y.; Zhang, Y. Severe surface ozone pollution in China: A global perspective. *Environ. Sci. Technol.* **2018**, *5*, 487–494.
21. Ma, S.; Shao, M.; Zhang, Y.; Dai, Q.; Xie, M. Sensitivity of $PM_{2.5}$ and O_3 pollution episodes to meteorological factors over the North China Plain. *Sci. Total Environ.* **2021**, *792*, 148474. [CrossRef] [PubMed]
22. Liu, J.; Wang, L.; Li, M.; Liao, Z.; Kulmala, M. Quantifying the impact of synoptic circulations on ozone variations in North China from April–October 2013–2017. *Atmos. Chem. Phys.* **2019**, *19*, 14477–14492. [CrossRef]
23. Liu, N.; Lin, W.; Ma, J.; Xu, W.; Xu, X. Seasonal variation in surface ozone and its regional characteristics at global atmosphere watch stations in China. *J. Environ. Sci.* **2019**, *77*, 291–302. [CrossRef] [PubMed]
24. Li, M.; Yao, Y.; Luo, D.; Zhong, L. The Linkage of the Large-Scale Circulation Pattern to a Long-Lived Heatwave over Mideastern China in 2018. *Atmosphere* **2019**, *10*, 89. [CrossRef]
25. Mao, J.; Wang, L.; Lu, C.; Liu, J.; Wang, Y. Meteorological mechanism for a large-scale persistent severe ozone pollution event over eastern China in 2017. *J. Environ. Sci.* **2020**, *92*, 187–199. [CrossRef]
26. Sicard, P.; Paoletti, E.; Agathokleous, E.; Araminien, V.; Marco, A.D. Ozone weekend effect in cities: Deep insights for urban air pollution control. *Environ. Res.* 2020, in press. [CrossRef]
27. Liu, H.; Deng, Y.; Huang, F.; Zhang, T.; Chen, Y. A study on the characteristics of ozone weekend effect and reaction sensitivity in Chengdu. *IOP Conf. Ser. Earth Environ. Sci.* **2020**, *467*, 012160. [CrossRef]
28. Xza, B.; Wzb, C.; Lh, B. Human activities and urban air pollution in Chinese mega city: An insight of ozone weekend effect in Beijing. *Phys. Chem. Earth Parts A/B/C* **2019**, *110*, 109–116.
29. Tang, W.; Zhao, C.; Geng, F.; Peng, L.; Zhou, G.; Gao, W.; Xu, J.; Tie, X. Study of ozone "weekend effect" in Shanghai. *Sci. China (Ser. D Earth Sci.)* **2008**, *51*, 1354–1360. [CrossRef]
30. Wang, S.; Zhao, Y.; Han, Y.; Li, R.; Fu, H.; Gao, S.; Duan, Y.; Zhang, L.; Chen, J. Spatiotemporal variation, source and secondary transformation potential of volatile organic compounds (VOCs) during the winter days in Shanghai, China. *Atmos. Environ.* **2022**, *286*, 119203. [CrossRef]
31. Zou, Y.; Charlesworth, E.; Yin, C.Q.; Yan, X.L.; Deng, X.J.; Li, F. The weekday/weekend ozone differences induced by the emissions change during summer and autumn in Guangzhou, China. *Atmos. Environ.* **2019**, *199*, 114–126. [CrossRef]
32. Minschwaner, K.; Salawitch, R.; McElroy, M. Absorption of solar radiation by O_2: Implications for O_3 and lifetimes of N_2O, $CFCl_3$, and CF_2Cl_2. *J. Geophys. Res. Atmos.* **1993**, *98*, 10543–10561. [CrossRef]
33. Bao, J.; Cao, J.; Gao, R.; Ren, Y.; Bi, F.; Wu, Z.; Chai, F.; Li, H. The prevention and control process, experience and enlightenment of ozone pollution in European ambient air to China. *Environ. Sci. Res.* **2021**, *34*, 890–901.

34. Sun, X.; Zhang, H.; Yao, Y.; Zhou, W.; Ouyang, Z.; Wang, X. Applicability of atmospheric ozone passive monitoring methods and correlation analysis of influencing factors. *Environ. Chem.* **2021**, *40*, 2747–2754.
35. Li, A.; Zhou, Q.; Xu, Q. Prospects for ozone pollution control in China: An epidemiological perspective. *Environ. Pollut.* **2021**, *285*, 117670. [CrossRef] [PubMed]
36. Monks, P.S.; Archibald, A.; Colette, A.; Cooper, O.; Coyle, M.; Derwent, R.; Fowler, D.; Granier, C.; Law, K.S.; Mills, G. Tropospheric ozone and its precursors from the urban to the global scale from air quality to short-lived climate forcer. *Atmos. Chem. Phys.* **2015**, *15*, 8889–8973.
37. Shen, J.; Huang, X.; Wang, Y.; Ye, S.; Pan, Y.; Chen, D.; Chen, H.; Qu, Y.; Lu, X.; Wang, Z. Characteristics and source analysis of ozone pollution in Guangdong Province. *J. Environ. Sci.* **2017**, *37*, 4449–4457.
38. Jia, H.; Yin, T.; Qu, X.; Cheng, N.; Cheng, B.; Wang, J.; Tang, W.; Meng, F.; Chai, F. Characteristics and source simulation of ozone concentration in Beijing and surrounding areas in 2015. *Environ. Sci. China* **2017**, *37*, 1231–1238.
39. Huang, Z.; Hong, L.; Yin, P.; Wang, X.; Zhang, Y. Study on the source of summer ozone pollution and the influence of atmospheric transport in Baoding. *J. Peking Univ. (Nat. Sci. Ed.)* **2018**, *54*, 665–672.
40. Ling, Z.; Guo, H.; Lam, S.; Saunders, S.; Wang, T. Atmospheric photochemical reactivity and ozone production at two sites in Hong Kong: Application of a master chemical mechanism–photochemical box model. *J. Geophys. Res. Atmos.* **2014**, *119*, 10567–10582. [CrossRef]
41. Cao, T.; Wu, K.; Kang, A.; Wen, X.; Li, H.; Wang, Y.; Lu, X.; Li, A.; Pan, W.; Fan, W. Analysis of ozone pollution characteristics and influencing factors in Chengdu-Chongqing urban agglomeration. *J. Environ. Sci.* **2018**, *38*, 1275–1284.
42. Dainius, J.; Vaida, V.; Renata, C.I.; Milda, P.I. Surface ozone concentration and its relationship with UV Radiation, Meteorological Parameters and Radon on the Eastern Coast of the Baltic Sea. *Atmosphere* **2016**, *7*, 27.
43. Deroubaix, A.; Brasseur, G.; Gaubert, B.; Labuhn, I.; Menut, L.; Siour, G.; Tuccella, P. Response of surface ozone concentration to emission reduction and meteorology during the COVID-19 lockdown in Europe. *Meteorol. Appl.* **2021**, *28*, e1990. [CrossRef]
44. Juráň, S.; Šigut, L.; Holub, P.; Fares, S.; Klem, K.; Grace, J.; Urban, O. Ozone flux and ozone deposition in a mountain spruce forest are modulated by sky conditions. *Sci. Total Environ.* **2019**, *672*, 296–304. [CrossRef] [PubMed]
45. Qi, J.; Mo, Z.; Yuan, B.; Huang, S.; Huangfu, Y.; Wang, Z.; Li, X.; Yang, S.; Wang, W.; Zhao, Y. An observation approach in evaluation of ozone production to precursor changes during the COVID-19 lockdown. *Atmos. Environ.* **2021**, *262*, 118618. [CrossRef] [PubMed]
46. Abdullah, S.; Nasir, N.H.A.; Ismail, M.; Ahmed, A.N.; Jarkoni, M.N.K. Development of ozone prediction model in urban area. *Int. J. Innov. Technol. Explor. Eng.* **2019**, *8*, 2263–2267. [CrossRef]
47. Wang, H.; Tan, Y.; Zhang, L.; Shen, L.; Zhao, T.; Dai, Q.; Guan, T.; Ke, Y.; Li, X. Characteristics of air quality in different climatic zones of China during the COVID-19 lockdown. *Atmos. Pollut. Res.* **2021**, *12*, 101247. [CrossRef]
48. Dang, R.; Liao, H.; Fu, Y. Quantifying the anthropogenic and meteorological influences on summertime surface ozone in China over 2012–2017. *Sci. Total Environ.* **2021**, *754*, 142394. [CrossRef] [PubMed]
49. Yu, Z.; Ma, J.; Mao, Z.; Cao, Y.; Qu, Y.; Xu, J. Analysis of meteorological conditions and weather classification of ozone pollution in Shanghai in 2017. *J. Meteorol. Environ.* **2019**, *35*, 46–54. [CrossRef]
50. Zhao, W.; Fan, S.; Guo, H.; Gao, B.; Sun, J.; Chen, L. Assessing the impact of local meteorological variables on surface ozone in Hong Kong during 2000–2015 using quantile and multiple line regression models. *Atmos. Environ.* **2016**, *144*, 182–193. [CrossRef]
51. Zhou, M.; Jiang, W.; Gao, W.; Zhou, B.; Liao, X. A high spatiotemporal resolution anthropogenic VOC emission inventory for Qingdao City in 2016 and its ozone formation potential analysis. *Process Saf. Environ. Prot.* **2020**, *139*, 147–160. [CrossRef]
52. Balzotti, C.; Briani, M.; De Filippo, B.; Piccoli, B. A computational modular approach to evaluate mahram NO_2 emissions and ozone production due to vehicular traffic. *Discret. Contin. Dyn. Syst.-B* **2022**, *27*, 3455. [CrossRef]
53. Zhang, H.; Han, L.; Ren, Y.; Yao, Y.; Sun, X.; Wang, X.; Zhou, W.; Hua, Z. Monitoring of the gradient movement of surface ozone concentration in urban and northwestern suburbs of Beijing. *Ecology* **2019**, *39*, 6803–6815.
54. Jing, S.; Ye, X.; Gao, Y.; Peng, Y.; Li, Y.; Wang, Q.; Shen, J.; Wang, H. The pollution characteristics and reactivity of volatile organic compounds during typical photochemical pollution in Hangzhou. *Environ. Sci.* **2020**, *41*, 3076–3084.
55. Botlaguduru, V.S.; Kommalapati, R.R.; Huque, Z. Long-term meteorologically independent trend analysis of ozone air quality at an urban site in the greater Houston area. *J. Air Waste Manag. Assoc.* **2018**, *68*, 1051–1064. [CrossRef] [PubMed]
56. Chen, W.; Chen, Y.; Chu, Y.; Zhang, J.; Xi, C.; Lin, C.; Feng, Z.; Lu, X. Numerical Simulation of Ozone Source Characteristics in the Pearl River Delta Region. *J. Environ. Sci.* **2022**, *42*, 293–308.
57. Qin, Y.; Liu, M.; Song, J.; Yu, R.; Li, L.; Su, J. The temporal and spatial variation characteristics of near-surface O_3 concentration in Guangdong-Hong Kong-Macao Greater Bay Area. *J. Environ. Sci.* **2021**, *41*, 2987–3000.
58. Atkinson, R. Atmospheric chemistry of VOCs and NO_x. *Atmos. Environ.* **2000**, *34*, 2063–2101. [CrossRef]
59. Wang, T.; Xue, L.; Brimblecombe, P.; Lam, Y.F.; Li, L.; Zhang, L. Ozone pollution in China: A review of concentrations, meteorological influences, chemical precursors, and effects. *Sci. Total Environ.* **2016**, *575*, 1582–1596. [CrossRef] [PubMed]
60. Chen, T.; Xue, L.; Zheng, P.; Zhang, Y.; Wang, W. Volatile organic compounds and ozone air pollution in an oil production region in northern China. *Atmos. Chem. Phys.* **2020**, *20*, 7069–7086. [CrossRef]
61. Xiaomeng, J.; Arlene, F.; Folkert, B.K.; De, S.I.; Lukas, V. Inferring Changes in Summertime Surface Ozone-NO_X-VOC Chemistry over U.S. Urban Areas from Two Decades of Satellite and Ground-Based Observations. *Environ. Sci. Technol.* **2021**, *54*, 6518–6529.

62. Liu, C.; Peng, R.; Du, X.; Zhang, Y.; Luo, X. Comparative research of meteorological conditions of typical dense fog and haze process over Pearl River Delta region. *Ecol. Environ. Sci.* **2019**, *28*, 1818–1828.
63. Yan, X.Y.; Hou, X.H.; Yang, Q.; Zhao, W.; Xu, Q.; Liu, Y.L. The variety of ozone and its relationship with meteorological conditions in typical cities in China. *Plateau Meteorol.* **2020**, *39*, 416–430.
64. Huang, J.; Liao, B.T.; Shen, Z.Q.; Zhang, Z.J.; Lan, J.; Wang, C.L. Research and application of boundary layer height based on microwave radiometer and aerosol lidar. *J. Trop. Meteorol.* **2022**, *38*, 180–192.
65. Song, L.; Deng, T.; Li, Z.L.; Wu, S.; He, G.W.; Li, F.; Wu, M.; Wu, D. Retrieval of boundary layer height and its influence on $PM_{2.5}$ concentration based on lidar observation over Guangzhou. *J. Trop. Meteorol. Engl. Ed.* **2021**, *27*, 303–318.
66. Levi, Y.; Dayan, U.; Levy, I.; Broday, D.M. On the association between characteristics of the atmospheric boundary layer and air pollution concentrations. *Atmos. Res.* **2020**, *231*, 104675.
67. Monks, P.S. A review of the observations and origins of the spring ozone maximum. *Atmos. Environ.* **2000**, *34*, 3545–3561. [CrossRef]
68. Yin, Y.; Shan, W.; Ji, X.; You, L.; Su, Y. Variation of atmospheric ozone concentration in Jinan. *Environ. Sci.* **2006**, *34*, 2299–2302.
69. Pan, C.; Zhu, X.; Wang, J.; Feng, X.; Shen, Q.; Xia, W.; Wan, P.; Qiu, F. Characteristics and influencing factors of ozone pollution in Yunnan Province in 2019. *Environ. Sci. Technol.* **2020**, *43*, 156–164.
70. Liu, Y.; Zhou, H.; Pei, Y.; Zhao, K.; Ren, Y. Characteristics of near-surface O_3 concentrations in Harbin. *J. Environ. Sci.* **2018**, *38*, 4454–4463.
71. Jenkin, M.E.; Clemitshawb, K.C. Ozone and other secondary photochemical pollutants: Chemical processes governing their formation in the planetary boundary layer. *Atmos. Environ.* **2000**, *34*, 2499–2527. [CrossRef]
72. Lili, L.; Wang, L.; Liu, X.; Wang, K.; Xu, Y.; Li, S.; Jiang, J. Spatial-temporal distribution characteristics of ozone and the relationship between meteorological factors in Harbin. *Environ. Sci. China* **2020**, *40*, 1991–1999.
73. Han, Z.; Zhang, M.; Hu, F. Numerical simulation of the effects of ecological NMHC on ozone and PAN. *J. Environ. Sci.* **2002**, *3*, 273–278.
74. Kerimray, A.; Azbanbayev, E.; Kenessov, B.; Plotitsyn, P.; Alimbayeva, D.; Karaca, F. Spatiotemporal variations and contributing factors of air pollutants in almaty, Kazakhstan. *Aerosol Air Qual. Res.* **2020**, *20*, 1340–1352. [CrossRef]
75. Carlsen, L.; Baimatova, N.; Kenessov, B.; Kenessova, O. Assessment of the Air Quality of Almaty. *Focus. Traffic Compon.* **2013**, *5*, 49–69.
76. Wu, Y.; Zhang, S.; Hao, J.; Liu, H.; Wu, X.; Hu, J.; Walsh, M.P.; Wallington, T.J.; Zhang, K.M.; Stevanovic, S. On-road vehicle emissions and their control in China: A review and outlook. *Sci. Total Environ.* **2017**, *574*, 332–349. [CrossRef] [PubMed]
77. Kerimray, A.; Bakdolotov, A.; Sarbassov, Y.; Inglezakis, V.; Poulopoulos, S. Air pollution in Astana: Analysis of recent trends and air quality monitoring system. *Mater. Today Proc.* **2018**, *5*, 22749–22758. [CrossRef]
78. Chang, J.H.-W.; Griffith, S.M.; Lin, N.-H. Impacts of land-surface forcing on local meteorology and ozone concentrations in a heavily industrialized coastal urban area. *Urban Clim.* **2022**, *45*, 101257. [CrossRef]
79. Wang, T.; Xue, L.; Feng, Z.; Dai, J.; Zhang, Y.; Tan, Y. Ground-level ozone pollution in China: A synthesis of recent findings on influencing factors and impacts. *Environ. Res. Lett.* **2022**, *17*, 063003. [CrossRef]
80. Chameides, W.; Fehsenfeld, F.; Rodgers, M.; Cardelino, C.; Martinez, J.; Parrish, D.; Lonneman, W.; Lawson, D.; Rasmussen, R.; Zimmerman, P. Ozone precursor relationships in the ambient atmosphere. *J. Geophys. Res. Atmos.* **1992**, *97*, 6037–6055. [CrossRef]
81. Tyagi, B.; Singh, J.; Beig, G. Seasonal progression of surface ozone and NO_X concentrations over three tropical stations in North-East India. *Environ. Pollut.* **2020**, *258*, 113662. [CrossRef] [PubMed]
82. Li, K.; Wang, H.; Chen, L.; Li, J.; Dong, F. Synergistic degradation of NO and C_7H_8 for inhibition of O_3 generation. *Appl. Catal. B Environ.* **2022**, *312*, 121423. [CrossRef]
83. Mao, J.; Yan, F.; Zheng, L.; You, Y.; Wang, W.; Jia, S.; Liao, W.; Wang, X.; Chen, W. Ozone control strategies for local formation-and regional transport-dominant scenarios in a manufacturing city in southern China. *Sci. Total Environ.* **2022**, *813*, 151883. [CrossRef] [PubMed]
84. Wang, X.; Yin, S.; Zhang, R.; Yuan, M.; Ying, Q. Assessment of summertime O_3 formation and the O_3-NO_X-VOC sensitivity in Zhengzhou, China using an observation-based model. *Sci. Total Environ.* **2022**, *813*, 152449. [CrossRef] [PubMed]